



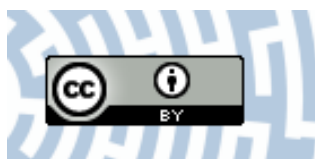
**You have downloaded a document from**  
**RE-BUŚ**  
**repository of the University of Silesia in Katowice**

**Title:** Transition metals (Cr<sup>3+</sup>) and lanthanides (Eu<sup>3+</sup>) in inorganic glasses with extremely different glass-formers B<sub>2</sub>O<sub>3</sub> and GeO<sub>2</sub>

**Author:** Karolina Kowalska, Marta Kuwik, Justyna Polak, Joanna Pisarska, Wojciech A. Pisarski

**Citation style:** Kowalska Karolina, Kuwik Marta, Polak Justyna, Pisarska Joanna, Pisarski Wojciech A. (2021). Transition metals (Cr<sup>3+</sup>) and lanthanides (Eu<sup>3+</sup>) in inorganic glasses with extremely different glass-formers B<sub>2</sub>O<sub>3</sub> and GeO<sub>2</sub>. "Materials" (2021), iss. 23, art. no. 7156, s. 1-15.

DOI: 10.3390/ma14237156



Uznanie autorstwa - Licencja ta pozwala na kopiowanie, zmienianie, rozprowadzanie, przedstawianie i wykonywanie utworu jedynie pod warunkiem oznaczenia autorstwa.



UNIwersYTET ŚLĄSKI  
W KATOWICACH





Biblioteka  
Uniwersytetu Śląskiego



Ministerstwo Nauki  
i Szkolnictwa Wyższego

Article

# Transition Metals ( $\text{Cr}^{3+}$ ) and Lanthanides ( $\text{Eu}^{3+}$ ) in Inorganic Glasses with Extremely Different Glass-Formers $\text{B}_2\text{O}_3$ and $\text{GeO}_2$

Karolina Kowalska \*, Marta Kuwik \*, Justyna Polak, Joanna Pisarska and Wojciech A. Pisarski

Institute of Chemistry, University of Silesia, Szkolna 9 Street, 40-007 Katowice, Poland; justyna.polak@us.edu.pl (J.P.); joanna.pisarska@us.edu.pl (J.P.); wojciech.pisarski@us.edu.pl (W.A.P.)  
\* Correspondence: karolina.kowalska@us.edu.pl (K.K.); marta.kuwik@us.edu.pl (M.K.)

**Abstract:** Glasses containing two different network-forming components and doped with optically active ions exhibit interesting properties. In this work, glass systems based on germanium dioxide and boron trioxide singly doped with lanthanides ( $\text{Eu}^{3+}$ ) and transition metals ( $\text{Cr}^{3+}$ ) ions are research subjects. Optical spectroscopy was the major research tool used to record excitation and emission spectra in a wide spectral range for studied systems. The emitted radiation of glasses doped with  $\text{Cr}^{3+}$  ions is dominated by broadband luminescence centered at 770 nm and 1050 nm ( ${}^4\text{T}_2 \rightarrow {}^4\text{A}_2$ ). Interestingly, the increase of concentration of one of the oxides contributed to the detectable changes of the R-line ( ${}^2\text{E} \rightarrow {}^4\text{A}_2$ ) of  $\text{Cr}^{3+}$  ions. Moreover, EPR spectroscopy confirmed the paramagnetic properties of the obtained glasses. The influence of molar ratio  $\text{GeO}_2:\text{B}_2\text{O}_3$  on spectroscopic properties for  $\text{Eu}^{3+}$  ions is discussed. The intensity of luminescence bands due to transitions of trivalent europium ions as well as the ratio R/O decrease with the increase of  $\text{B}_2\text{O}_3$ . On the other hand, the increase in concentration  $\text{B}_2\text{O}_3$  influences the increasing tendency of luminescence lifetimes for the  ${}^5\text{D}_0$  state of  $\text{Eu}^{3+}$  ions. The results will contribute to a better understanding of the role of the glass host and thus the prospects for new optical materials.

**Keywords:** glasses; network-former; luminescence properties; red-emitting materials; paramagnetic ions



**Citation:** Kowalska, K.; Kuwik, M.; Polak, J.; Pisarska, J.; Pisarski, W.A. Transition Metals ( $\text{Cr}^{3+}$ ) and Lanthanides ( $\text{Eu}^{3+}$ ) in Inorganic Glasses with Extremely Different Glass-Formers  $\text{B}_2\text{O}_3$  and  $\text{GeO}_2$ . *Materials* **2021**, *14*, 7156. <https://doi.org/10.3390/ma14237156>

Academic Editors: Andrea Piccolroaz and A. Javier Sanchez-Herencia

Received: 9 September 2021

Accepted: 19 November 2021

Published: 24 November 2021

**Publisher's Note:** MDPI stays neutral with regard to jurisdictional claims in published maps and institutional affiliations.



**Copyright:** © 2021 by the authors. Licensee MDPI, Basel, Switzerland. This article is an open access article distributed under the terms and conditions of the Creative Commons Attribution (CC BY) license (<https://creativecommons.org/licenses/by/4.0/>).

## 1. Introduction

In recent years, the field of engineering materials (including glasses) has evolved, introducing new information about the interesting properties of systems [1–3]. Glass is a material characterized by a lack of long-range order with no defined glass transition temperature [4]. In an excellent communication [5], Zanotto and Mauro declared that a comprehensive definition of glass, combining the aspect of knowledge improvement and modernity, is still being explored. Interestingly, to this day, the technology to prepare glass is based on substances such as  $\text{SiO}_2$ ,  $\text{B}_2\text{O}_3$ ,  $\text{GeO}_2$ ,  $\text{P}_2\text{O}_5$ , which are the only ones that meet Zachariasen's rules for glass formation [6]. A variety of modifications in the chemical composition of glasses enables the introduction of different optically active ions such as transition metal and rare-earth ions. This allows obtaining unique luminescent properties and developing new optical materials operating in a wide spectral range. The glass systems are applied in light-emitting diodes, lasers, phosphors, or optical amplifiers [7–9]. In defining the spectroscopic properties of amorphous materials, a significant contribution is the composition of the glass matrices. In particular, the type and concentration of the network-former and/or network-modifier influence structural [10,11], thermal [12], and optical properties [13–15]. Recently, Jiao et al. [16] presented that increasing the boron oxide ratio visibly improves the luminescence characterizations of  $\text{Sm}^{3+}$ ,  $\text{Dy}^{3+}$ , and  $\text{Tb}^{3+}$  ions in glass systems. However, the wide range of compositional modifications presented for silicate glasses containing different network modifier oxides [17] indicated significant differences in the local surroundings of  $\text{Eu}^{3+}$  ions. Very satisfactory results of analysis

of luminescence decay kinetics were also obtained for phosphate glasses. The value of measured lifetime for  ${}^4F_{3/2}$  level of  $\text{Nd}^{3+}$  ions increased to 2.49 ms with changing the glass composition [18].

The number of publications indicates that among various inorganic systems, borate glasses are preferred for the luminescent centers due to their spectroscopic properties [19]. Divina et al. [20] carried out spectroscopic studies of alkali lead-bismuth borate glasses doped with  $\text{Dy}^{3+}$  ions. It was reported that these systems exhibit yellowish-white luminescence and suggested the utility for w-LED applications. Borate glasses can also be useful for infrared emitting device applications due to intense near-infrared emission at 1056 nm corresponding to the  ${}^4F_{3/2} \rightarrow {}^4I_{11/2}$  transition of  $\text{Nd}^{3+}$  ions [21]. However, these glasses are characterized by high phonon energy (1300–1500  $\text{cm}^{-1}$ ), and it could have a negative effect on the photoluminescence properties of systems doped with rare-earth ions [22]. On the other hand, it limits their application potential in photonic applications. Therefore, it is preferable to introduce other oxides to the host matrix to reduce the probability of non-radiative transitions. Germanate glasses have been of great interest for many years because of the specificity of their physical properties, such as glass transition temperature, particularly [23]. Moreover, germanate glass systems exhibit the ability to absorb X-rays and high transparency in the near-infrared spectral region [24]. These systems have unique properties such as low phonon energy ( $\sim 800 \text{ cm}^{-1}$ ), good thermal stability, and good lanthanide ions solubility [25]. The results obtained in our previous works [26] proved that the developed glasses containing germanate (IV) oxide and titanate (IV) oxide determine the differences in the profile of the registered luminescence bands of d-transition metal and rare-earth ions. The present paper presents the correlation between the content of two different glass-network formers ( $\text{GeO}_2$  and  $\text{B}_2\text{O}_3$ ) and the spectroscopic properties of inorganic glasses singly doped with transition metal ions ( $\text{Cr}^{3+}$ ) and lanthanide ions ( $\text{Eu}^{3+}$ ).

The spectroscopic properties of rare-earth and transition metal ions in materials are subject to rigorous interpretation that provides important contributions to contemporary scientific investigations. The luminescence spectra of  $\text{Eu}^{3+}$  ions are characterized by f–f transitions [27,28], respectively. The first observation of these transitions dates from 1901 by Demarcay, considered the discoverer of the europium ion [29]. According to the work of Binnemans [30], the relative intensities of transitions in emission spectra can be used to probe the local environment around  $\text{Eu}^{3+}$  ions. Analysis of the properties of glass systems can also be spectroscopically monitored by trivalent chromium ions [31]. Modification of the quantitative relationship of glass-former and glass-modifier oxides causes them to occupy different sites with different crystal field strengths [32,33]. Moreover, the laser transition  ${}^4T_2 \rightarrow {}^4A_2$  of  $\text{Cr}^{3+}$  ions is very sensitive to its chemical environment.

Based on these criteria, a series of glasses with the following chemical formula  $\text{GeO}_2\text{-B}_2\text{O}_3\text{-BaO-Ga}_2\text{O}_3\text{-Cr}_2\text{O}_3$  and  $\text{GeO}_2\text{-B}_2\text{O}_3\text{-BaO-Ga}_2\text{O}_3\text{-Eu}_2\text{O}_3$  were synthesized. The glass systems were obtained using the conventional high-temperature melt-quenching technique of high-purity metal oxides as starting materials. The selected optically active ions have a special role in the research because they are useful spectroscopic probes. For this reason, the structural properties of glasses doped with  $\text{Cr}^{3+}$  ions were investigated using electron paramagnetic resonance spectroscopy. The luminescence characterization of this study was aimed at determining which of the glass-network oxides favorably influence the optical properties of the obtained glasses. Excitation and emission spectra in the visible and near-infrared ranges were recorded. In particular, spectroscopic features such as R-line luminescence, superimposed on the broad emission band  ${}^4T_2 \rightarrow {}^4A_2$  transition of chromium ions, were analyzed. On the other hand, a fluorescence intensity ratio (R/O) parameter as a function of  $\text{GeO}_2\text{:B}_2\text{O}_3$  concentration was estimated of  ${}^5D_0 \rightarrow {}^7F_J$  ( $J = 1\text{--}2$ ) transitions of europium ions. Moreover, luminescence lifetimes for the upper  ${}^5D_0$  excited level of  $\text{Eu}^{3+}$  ions are evaluated and discussed.

## 2. Materials and Methods

### 2.1. Glass Synthesis

In the present work, a series of inorganic glasses were synthesized using a high-temperature melt quenching-technique. The appropriate amounts of anhydrous metal oxides: germanium (IV) oxide (Sigma-Aldrich Chemical Co., St. Louis, MO, USA,  $\geq 99.99\%$ ), boron trioxide (Sigma-Aldrich Chemical Co., St. Louis, MO, USA, 99.98%), barium oxide (Sigma-Aldrich Chemical Co., St. Louis, MO, USA, 99.99%), gallium (III) oxide (Sigma-Aldrich Chemical Co., St. Louis, MO, USA,  $>99.99$ ), chromium (III) oxide (Sigma-Aldrich Chemical Co., St. Louis, MO, USA, 99.9%), europium (III) oxide (Sigma-Aldrich Chemical Co., St. Louis, MO, USA, 99.99%), were carefully homogenized in an agate mortar. Melting of the desired mixtures in corundum crucibles was carried out in an electric furnace in an air atmosphere at the temperature of 1250 °C. The glass samples were kept at this temperature for 1 h before slowly cooled down to room temperature. Then the samples were subjected to grinding and polishing treatment. Based on X-ray diffraction measurements it has been confirmed that all samples are fully amorphous. As a result of the above synthesis procedure, two series of glass samples doped with transition metal ( $\text{Cr}^{3+}$ ) and lanthanide ( $\text{Eu}^{3+}$ ) ions were obtained (Tables 1 and 2).

**Table 1.** Chemical compositions (mol%) of glass samples doped with transition metal ( $\text{Cr}^{3+}$ ) ions.

Sample Code	$\text{GeO}_2$	$\text{B}_2\text{O}_3$	BaO	$\text{Ga}_2\text{O}_3$	$\text{Cr}_2\text{O}_3$
Cr59:1	59	1	30	9.75	0.25
Cr11:1	55	5	30	9.75	0.25
Cr5:1	50	10	30	9.75	0.25
Cr2:1	40	20	30	9.75	0.25
Cr1:1	30	30	30	9.75	0.25
Cr1:2	20	40	30	9.75	0.25
Cr1:5	10	50	30	9.75	0.25

**Table 2.** Chemical compositions (mol%) of glass samples doped with lanthanides ( $\text{Eu}^{3+}$ ) ions.

Sample Code	$\text{GeO}_2$	$\text{B}_2\text{O}_3$	BaO	$\text{Ga}_2\text{O}_3$	$\text{Eu}_2\text{O}_3$
Eu59:1	59	1	30	9.75	0.25
Eu11:1	55	5	30	9.75	0.25
Eu5:1	50	10	30	9.75	0.25
Eu2:1	40	20	30	9.75	0.25
Eu1:1	30	30	30	9.75	0.25
Eu1:2	20	40	30	9.75	0.25
Eu1:5	10	50	30	9.75	0.25

### 2.2. Characterization Techniques

We used the following research tools to characterize the sample properties: electron paramagnetic resonance (EPR) spectroscopy and optical spectroscopy. EPR spectroscopy was used to describe the composition of glasses doped with transition metal ions ( $\text{Cr}^{3+}$ ). Each glass sample in powdered form was placed inside a special quartz tube. EPR spectra were recorded using Bruker EMX EPR spectrometer (Bruker-Biospin, Karlsruhe, Germany) operating at X-band frequency (9.8 GHz) with a modulation amplitude of 2.0 G. The magnetic field was scanned from 1000 G to 5000 G. The EPR instrument parameters are as follows: central field 3480 G, time constant 40.96, gain  $1 \times 10^4$  G, microwave power 20.12 mW.

The optical properties of glasses were analyzed using luminescence spectroscopy with the system PTI QuantaMaster QM 40 UV/VIS Steady State Spectrofluorometer (Photon Technology International, Birmingham, NJ, USA). The laser equipment was coupled with

a tunable pulsed optical parametric oscillator (OPO), pumped by the third harmonic of a Nd:YAG laser (Opotek Opolette 355 LD, Carlsbad, CA, USA). The system consisted of a double 200 mm monochromators, a xenon lamp as a light source, a multimode UV-VIS PMT (R928) (PTI Model 914), and Hamamatsu H10330B-75 (Hamamatsu, Bridgewater, NJ, USA) detectors, PTI, and ASOC-10 USB-2500 oscilloscope. Resolution for spectral measurements (excitation and emission spectra) was  $\pm 0.25$  nm ( $\text{Cr}^{3+}$ -doped glass samples) and  $\pm 0.5$  nm ( $\text{Eu}^{3+}$ -doped glass samples), whereas decay curves with accuracy  $0.5 \mu\text{s}$  were acquired. All measurements were performed at room temperature.

### 3. Results and Discussion

#### 3.1. Transition Metals— $\text{Cr}^{3+}$

Electron paramagnetic resonance (EPR) is a significant experimental technique for determining the environment of transition metal ( $\text{Cr}^{3+}$ ) ions in glasses. Analysis of EPR spectra gives information about the glass network and symmetry around transition metal ions. Figure 1 presents electron paramagnetic resonance spectra of glassy systems containing two types of glass-formers and doped with  $\text{Cr}^{3+}$  ions. Independently on the molar ratio  $\text{GeO}_2:\text{B}_2\text{O}_3$ , the similar registered EPR spectra show one signal at a low magnetic field and one resonance line at a high magnetic field.

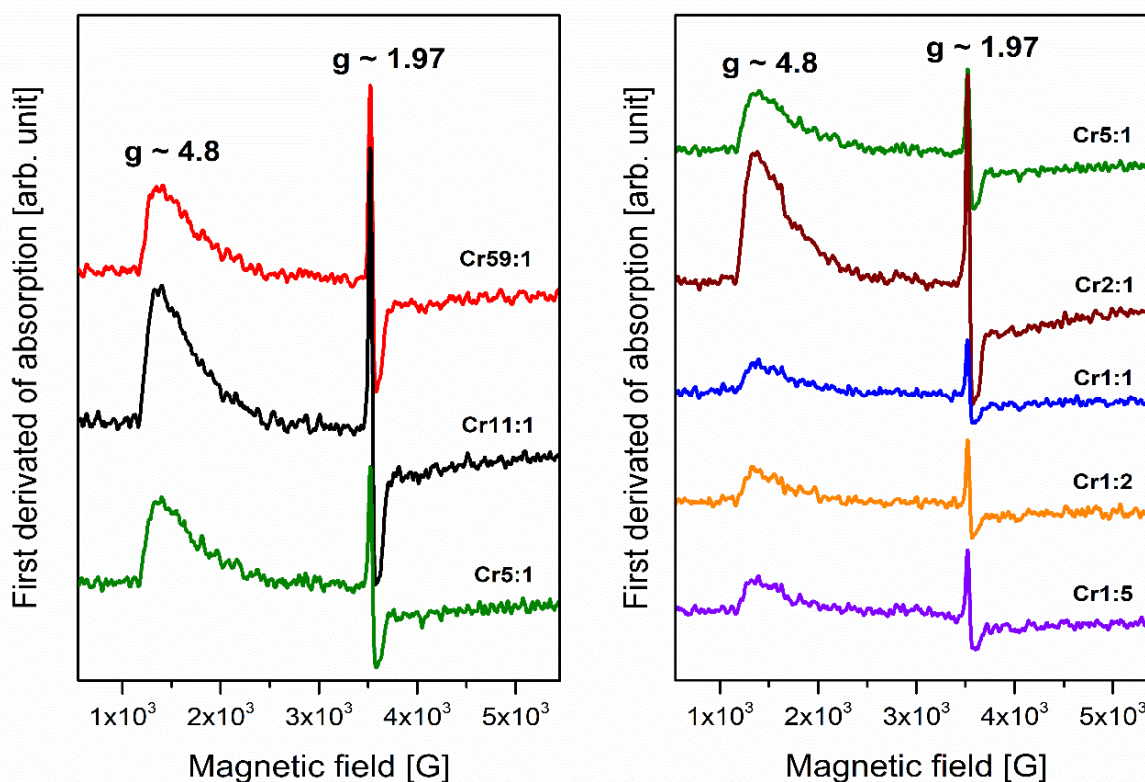


**Figure 1.** Electron paramagnetic resonance spectra of  $\text{Cr}^{3+}$  ions doped glass samples with different concentrations of glass-former components ( $\text{GeO}_2$  and  $\text{B}_2\text{O}_3$ ).

The broad asymmetric signal with  $g$  value  $\sim 4.8$  corresponds to isolated  $\text{Cr}^{3+}$  centers in strongly distorted octahedral sites [34]. On the other hand, the narrow resonance line with  $g$  close to 1.97 is assigned to exchange-coupled  $\text{Cr}^{3+}\text{-Cr}^{3+}$  pairs [35], or this signal can be attributed to the trivalent chromium ions in cubic sites of the glass network [36]. The similar measured effective  $g$  values obtained for studied glasses were also noticed for  $\text{Cr}^{3+}$  ions in  $\text{CdO-SrO-B}_2\text{O}_3\text{-SiO}_2$  [37],  $\text{ZnO-As}_2\text{O}_3\text{-Sb}_2\text{O}_3$  [38], and  $\text{Li}_2\text{CO}_3\text{-B}_2\text{O}_3\text{-P}_2\text{O}_5$  systems [39].

The intensity of the signals is higher for glasses with a dominant concentration of glass-former  $\text{GeO}_2$  (samples from Cr59:1 to Cr2:1). However, the intensity of resonance lines is lower for samples with increasing content of glass-former  $\text{B}_2\text{O}_3$ . Apart from the variation in signal intensity, no important modifications were observed when the glass-formers concentrations in glass composition changed. The influence of glass-formers on the spectral properties of systems doped with  $\text{Cr}^{3+}$  ions was studied. To this goal, the excitation spectra were monitored at  $\lambda_{\text{em}} = 780 \text{ nm}$  (Figure 2), and two broad bands were observed due to transitions from the  $^4\text{A}_2$  ground level of trivalent chromium ions. From the literature, it is well known that  $\text{Cr}^{3+}$  ions have strong visible absorption due to the spin-allowed but parity-forbidden transitions [32].

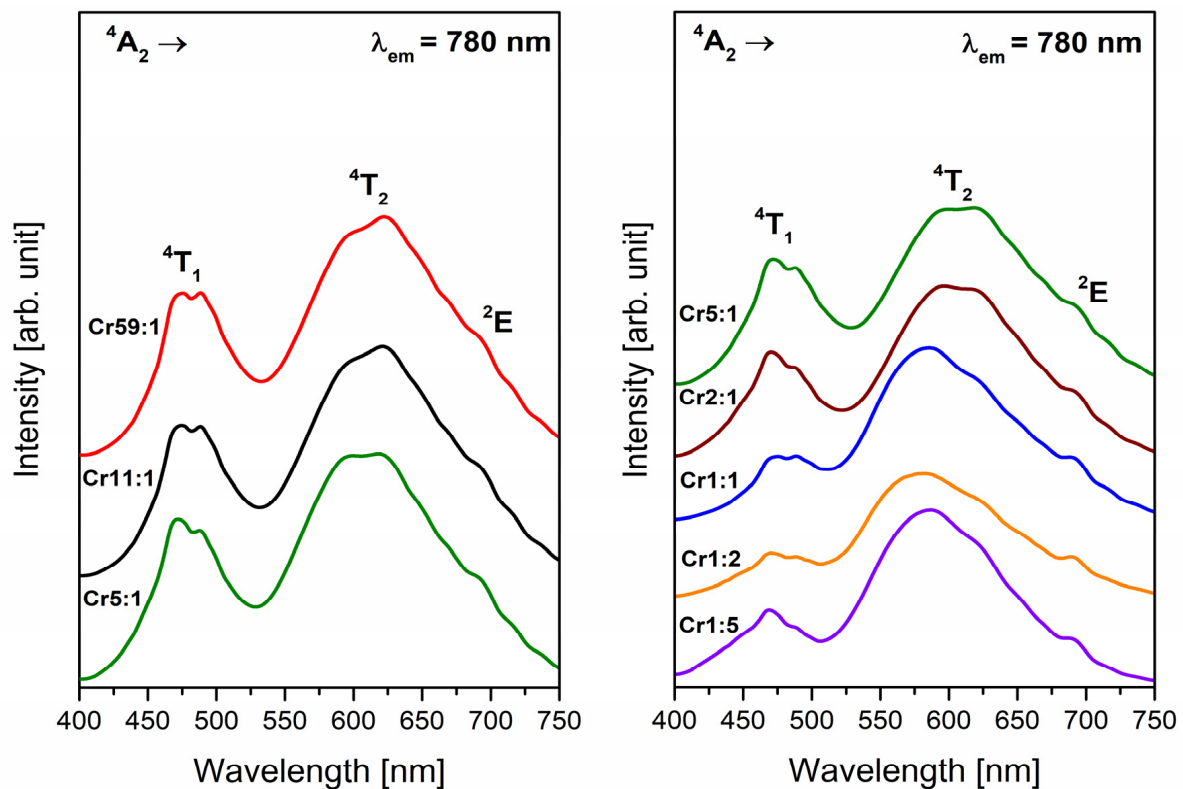


**Figure 2.** Excitation spectra of  $\text{Cr}^{3+}$  ions doped glass samples with different concentrations of glass-former components ( $\text{GeO}_2$  and  $\text{B}_2\text{O}_3$ ) monitored at 780 nm.

The first excitation band around at 480 nm corresponds to the transition  $^4\text{A}_2 \rightarrow ^4\text{T}_1$  of  $\text{Cr}^{3+}$  ions. In contrast, the second band consists of three overlapped peaks located at 600 nm, 625 nm, 690 nm and related to transitions originating from ground level to the  $^4\text{T}_2$ ,  $^2\text{T}_1$ , and  $^2\text{E}$  excited levels of  $\text{Cr}^{3+}$  ions, respectively. It is worth noting that the intensity of band maxima of the  $^4\text{A}_2 \rightarrow ^4\text{T}_2$  and  $^4\text{A}_2 \rightarrow ^2\text{T}_1$  transitions change with the molar ratio of glass-formers ( $\text{GeO}_2:\text{B}_2\text{O}_3$ ). The intensity of the band corresponding to the transition  $^4\text{A}_2 \rightarrow ^4\text{T}_2$  of  $\text{Cr}^{3+}$  ions increases when the content of germanium dioxide decreases. On the other hand, the intensity of band attributed to excitation level  $^2\text{T}_1$  is the highest for system Cr59:1 and the lowest for glass sample Cr1:5. The effect of changing the glass composition on the intensity of excitation bands was also observed for borate glass-ceramics with a constant concentration of trivalent chromium ions [40]. Moreover, the analysis of excitation spectra indicates that the forbidden electron transition  $^4\text{A}_2 \rightarrow ^2\text{E}$  of  $\text{Cr}^{3+}$  ions is more clearly separated for glasses with a higher concentration of boron trioxide as glass-former (Cr1:1, Cr1:2, Cr1:5). To study the luminescence properties of systems with both glass-formers ( $\text{GeO}_2$  and  $\text{B}_2\text{O}_3$ ), the wavelength  $\lambda = 600 \text{ nm}$  was chosen for registration emission spectra.

Figures 3 and 4 show luminescence spectra registered in the red and near-infrared spectral region. The band located in the range 650–850 nm with a maximum at about 780 nm indicates that all samples exhibit red luminescence irrespective of the molar ratio of glass-formers. The presence of this broad emission band confirms results from analysis of EPR spectra and proves that trivalent chromium ions are in octahedral sites [41]. It is interesting to see that the band is a result of overlapping two transitions of  $\text{Cr}^{3+}$  ions: allowed  ${}^4\text{T}_2 \rightarrow {}^4\text{A}_2$  and forbidden  ${}^2\text{E} \rightarrow {}^4\text{A}_2$ . The broad band corresponds to allowed transition, and it is attributed to the  $\text{Cr}^{3+}$  centers in low-field sites [42]. However, the narrow emission band corresponding  ${}^2\text{E} \rightarrow {}^4\text{A}_2$  transition called R-line suggests that chromium ions are subjected to high-field sites [43]. The appearance of the two luminescence bands proves the existence of both octahedral sites. Therefore, some of the  $\text{Cr}^{3+}$  ions emit from the  ${}^4\text{T}_2$  level and some from the  ${}^2\text{E}$  level [44].

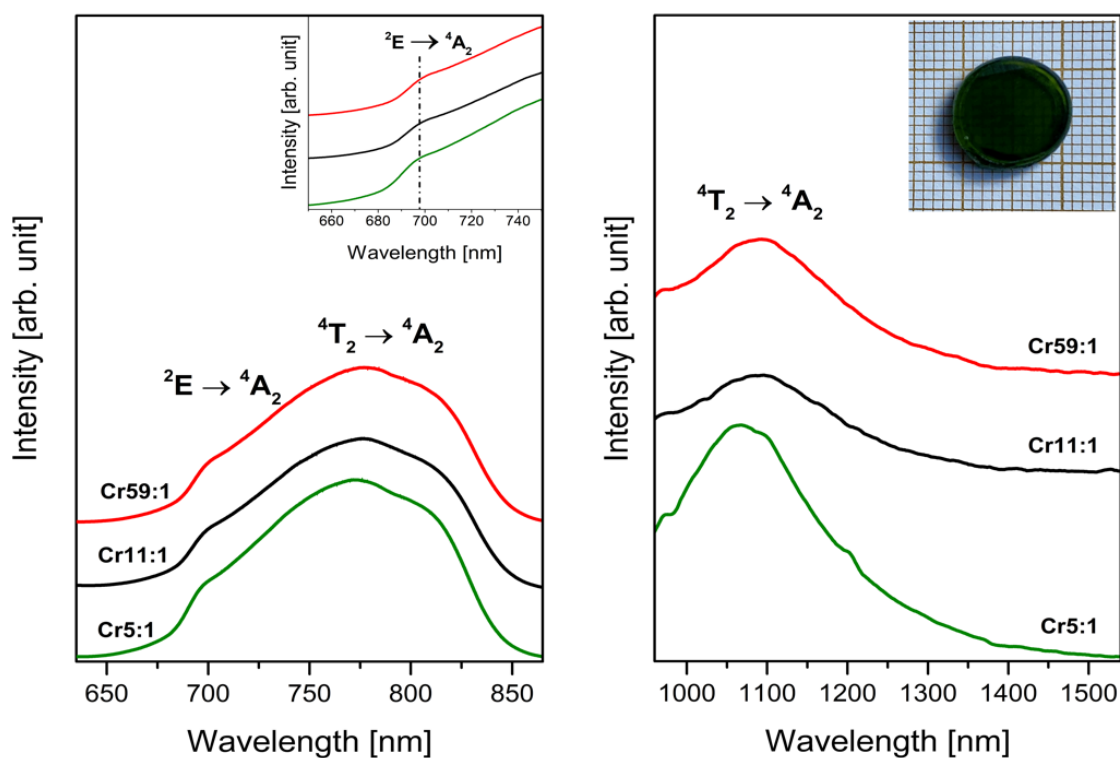


**Figure 3.** Emission spectra of  $\text{Cr}^{3+}$  ions doped glass samples (Cr59:1, Cr11:1, Cr5:1) with different concentrations of glass-former components ( $\text{GeO}_2$  and  $\text{B}_2\text{O}_3$ ). Insets show an enlargement of the emission spectrum corresponding to the R-line and a photographic image of a glass sample doped with  $\text{Cr}^{3+}$  ions.

The shape of emission resulting from trivalent chromium ions occupying different sites was changed with molar ratio  $\text{GeO}_2:\text{B}_2\text{O}_3$ . The intensity of R-line increases with decreasing concentration of glass-former  $\text{GeO}_2$  in studied systems. It was clearly observed for sample Cr5:1 with weak R-line and sample Cr1:5 with intense narrow emission band (Figure 4). The region 680–700 nm, where the R-line is situated, shows that the spectral lines are slightly shifted toward lower wavelengths with increasing  $\text{B}_2\text{O}_3$  concentration. Simultaneously, the intensity of the broad band related to transition originating from excited level  ${}^4\text{T}_2$  to the ground level  ${}^4\text{A}_2$  of  $\text{Cr}^{3+}$  ions decreases with changing of glass-formers concentration. However, it is still the dominant emission for  $\text{Cr}^{3+}$  ions in studied systems. The blue shift of the maximum of this emission band was also stated ( $\lambda_{\text{max}} = 773$  nm and  $\lambda_{\text{max}} = 753$  nm for Cr59:1 and Cr1:5 sample, respectively). According to Narendrudu et al. [45] changing the intensity of transitions  ${}^4\text{T}_2 \rightarrow {}^4\text{A}_2$  and  ${}^2\text{E} \rightarrow {}^4\text{A}_2$  of trivalent chromium ions can be related to the energy transfer between isolated  $\text{Cr}^{3+}$  centers and coupled  $\text{Cr}^{3+}-\text{Cr}^{3+}$  pairs. Furthermore, Yang et al. [46] reported that the substitution of  $\text{BaF}_2$  in germanate glasses causes enhance broad emission attributed to the  ${}^4\text{T}_2 \rightarrow {}^4\text{A}_2$

transition of trivalent chromium ions. Our results indicate that luminescence emitted by  $\text{Cr}^{3+}$  ions in studied systems depends on glass composition. Especially, different glass-formers influence the shape and intensity of emission corresponding to transitions of  $\text{Cr}^{3+}$  ions. It can be concluded that low-field sites are occupied by the greater part of trivalent chromium ions in samples Cr5:1, Cr11:1, Cr5:1, and Cr2:1 than in glasses with higher  $\text{B}_2\text{O}_3$  concentration. On the contrary, more  $\text{Cr}^{3+}$  ions are located in high-field sites in glass systems Cr1:2 and Cr1:5 than in samples with dominant content of  $\text{GeO}_2$  as glass-former.

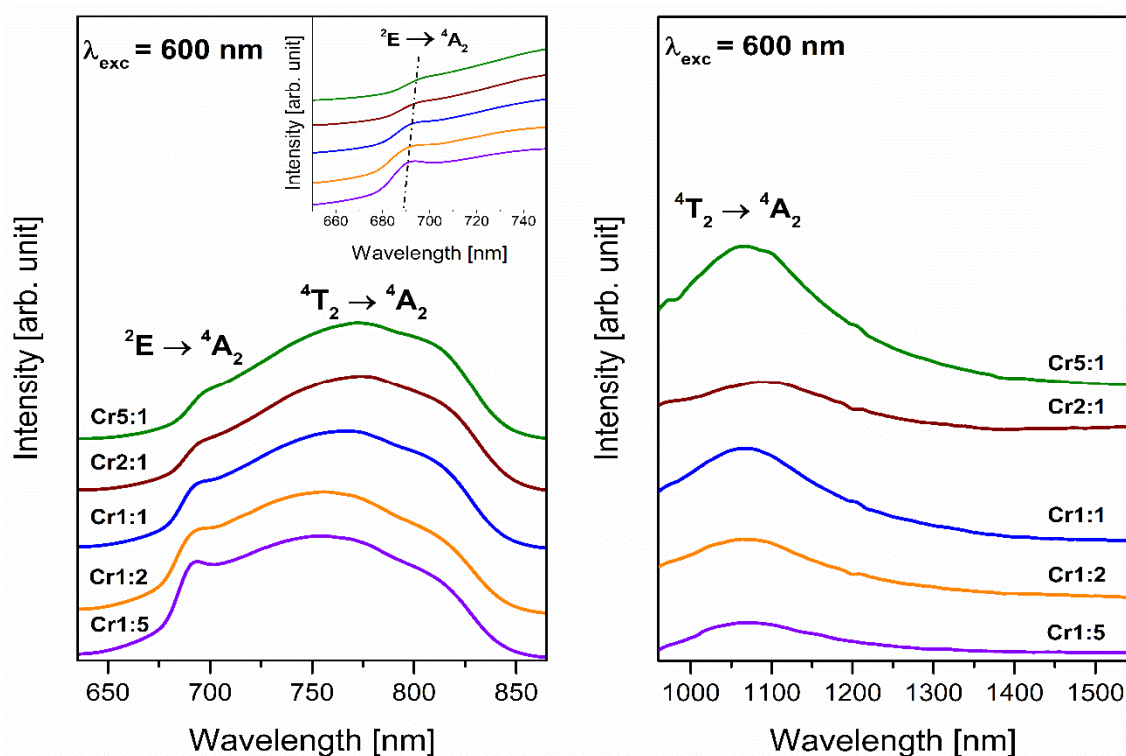


**Figure 4.** Emission spectra of  $\text{Cr}^{3+}$  ions doped glass samples (Cr5:1, Cr2:1, Cr1:1, Cr1:2, Cr1:5) with different concentrations of glass-former components ( $\text{GeO}_2$  and  $\text{B}_2\text{O}_3$ ). The inset is an enlargement of the emission spectrum corresponding to the R-line of  $\text{Cr}^{3+}$  ions.

Near-infrared spectra for glass samples with two glass-formers present one luminescence band in the 1000–1400 nm spectral region. Similar emission was observed for lithium, and lithium potassium borate systems and the broad registered band was assigned to transition from the  ${}^4\text{T}_2$  level to the  ${}^4\text{A}_2$  ground level of trivalent chromium ions [47]. Previously published results by Li et al. [48] indicate the luminescence centered at about 1030 nm corresponds to the  ${}^4\text{T}_2 \rightarrow {}^4\text{A}_2$  transition in tetrahedral sites of  $\text{Cr}^{3+}$  ions. For that reason, we can conclude that both emission bands with maxima at about 780 nm and 1070 nm are related to the same transition of trivalent chromium ions. However, red luminescence is attributed to  $\text{Cr}^{3+}$  ions in octahedral sites, and near-infrared emission corresponds to trivalent chromium ions in tetrahedral sites. The molar ratio  $\text{GeO}_2:\text{B}_2\text{O}_3$  influences the intensity of emission but significant differences in the shape of spectra were not observed.

### 3.2. Lanthanides— $\text{Eu}^{3+}$

Next, we undertook the characterization of the optical properties for the obtained glass samples doped with europium ions by recording the excitation spectra shown in Figure 5. The excitation spectra were registered in the spectral range from 350 to 500 nm and monitored at 611 nm, the wavelength corresponding to the red emission of the  ${}^5\text{D}_0 \rightarrow {}^7\text{F}_2$  transition of  $\text{Eu}^{3+}$  ions.



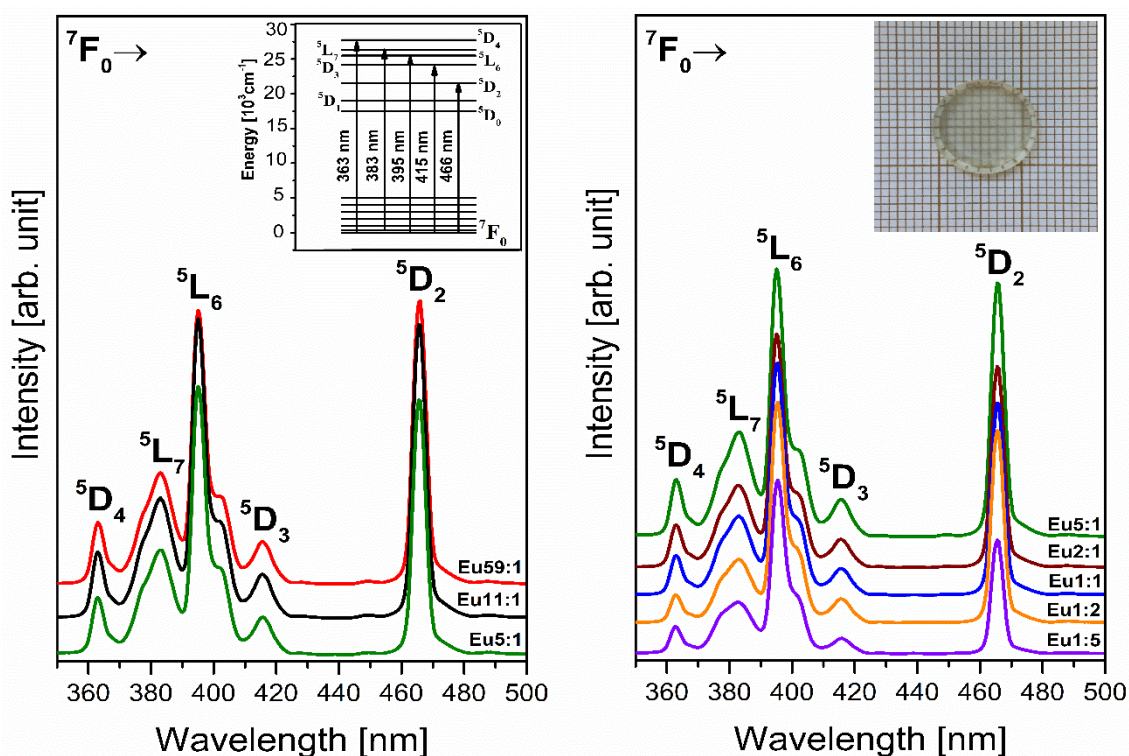


**Figure 5.** Excitation spectra of  $\text{Eu}^{3+}$  ions doped glass samples with different concentrations of glass-former components ( $\text{GeO}_2$  and  $\text{B}_2\text{O}_3$ ) monitored at 611 nm. Insets show the energy level diagram of trivalent europium ions and a photographic image of a glass sample doped with  $\text{Eu}^{3+}$  ions.

The spectra show the occurrence of bands associated with typical  $4f^6-4f^6$  intra-configuration electronic transitions of trivalent europium ions, which can be attributed to individual transitions from the ground state  ${}^7F_0$  to higher excited states of  $\text{Eu}^{3+}$  ions [49]. In the analyzed spectral range, bands centered at 363 nm ( ${}^7F_0 \rightarrow {}^5D_4$ ), 383 nm ( ${}^7F_0 \rightarrow {}^5L_7$ ), 396 nm ( ${}^7F_0 \rightarrow {}^5L_6$ ), 415 nm ( ${}^7F_0 \rightarrow {}^5D_3$ ), and 466 nm ( ${}^7F_0 \rightarrow {}^5D_2$ ), were recorded. Preliminary observations of the excitation spectra clearly demonstrated that the intensity of individual bands depends on the molar ratio  $\text{GeO}_2:\text{B}_2\text{O}_3$ . By considering the three glass samples Eu1:5, Eu5:1, and Eu59:1, it was concluded that increasing the germanium dioxide content contributes to a gradual increase of the intensity. However, among registered excitation bands, the most intense correspond to  ${}^7F_0 \rightarrow {}^5L_6$  (396 nm) and  ${}^7F_0 \rightarrow {}^5D_2$  (466 nm) transitions of trivalent europium ions, regardless of the molar ratio  $\text{GeO}_2:\text{B}_2\text{O}_3$ . According to the results obtained for glasses based on germanium dioxide, the intensity ratio of these excitation bands significantly depends on the glass composition. Ramesh et al. [50] showed that in germanate glasses with  $\text{PbO}$  the bands related to  ${}^7F_0 \rightarrow {}^5L_6$  and  ${}^7F_0 \rightarrow {}^5D_2$  transitions of  $\text{Eu}^{3+}$  ions are equally intense. On the other hand, for the same glass systems where  $\text{PbO}$  was replaced by  $\text{Bi}_2\text{O}_3$ , the intensity of the band located at 464 nm ( ${}^7F_0 \rightarrow {}^5D_2$ ) is two times stronger than that centered at 393 nm ( ${}^7F_0 \rightarrow {}^5L_6$ ). Obtained results indicate that the intensity of the excitation bands attributed to  ${}^7F_0 \rightarrow {}^5L_6$  and  ${}^7F_0 \rightarrow {}^5D_2$  transitions of  $\text{Eu}^{3+}$  ions is similar for system Eu59:1. In contrast, the increase of concentration of boron trioxide causes the decreasing intensity of the band corresponding to the  ${}^7F_0 \rightarrow {}^5D_2$  transition. Additionally, as a function of the concentration of the glass-formers, any spectral shifts were not observed. It is well known that the sharp excitation wavelength gives the intense emission. Hence, bands related to the  ${}^7F_0 \rightarrow {}^5L_6$  and  ${}^7F_0 \rightarrow {}^5D_2$  transitions suggest a potential for effective optical excitation of amorphous materials containing  $\text{Eu}^{3+}$  ions. For this reason, we chose a wavelength  $\lambda_{\text{exc}} = 396$  nm in the luminescence investigations, to demonstrate the suitability of the obtained glasses for lighting applications.

The main role analysis of emission and functional properties of the glasses doped with lanthanides ions is the characterization of the emitted radiation, which results from the electron transitions of  $\text{Ln}^{3+}$  ions [51]. Noticeably, the most significant point of the studies of systems containing trivalent europium ions is to obtain efficient red emission. It is known that the excitation energy of the  $\text{Eu}^{3+}$  ions is transferred non-radiatively from excited levels  $^5\text{L}_6$ ,  $^5\text{D}_3$ ,  $^5\text{D}_2$ , and  $^5\text{D}_1$  to the energy level  $^5\text{D}_0$ . Then the energy transfers back to the ground state causing characteristic visible emissions corresponding to the  $^5\text{D}_0 \rightarrow ^7\text{F}_j$  transitions (where  $J = 0-6$ ) of  $\text{Eu}^{3+}$  ions [52–54]. The emission spectra in the visible range under xenon lamp excitation for the obtained glasses were recorded and five well-separated bands were observed. According to the energy level scheme of  $\text{Eu}^{3+}$  ions, the registered emission bands presented in Figure 6 correspond to the transitions from the excited level  $^5\text{D}_0$  to the lower-lying levels  $^7\text{F}_0$ ,  $^7\text{F}_1$ ,  $^7\text{F}_2$ ,  $^7\text{F}_3$ , and  $^7\text{F}_4$  were assigned using the references [55,56]. The presented spectra demonstrate that the intensity of the luminescence band at 611 nm attributed to the red emission of europium ions increases two times when the molar ratio  $\text{GeO}_2:\text{B}_2\text{O}_3$  increases in the direction from 1:5 to 5:1.

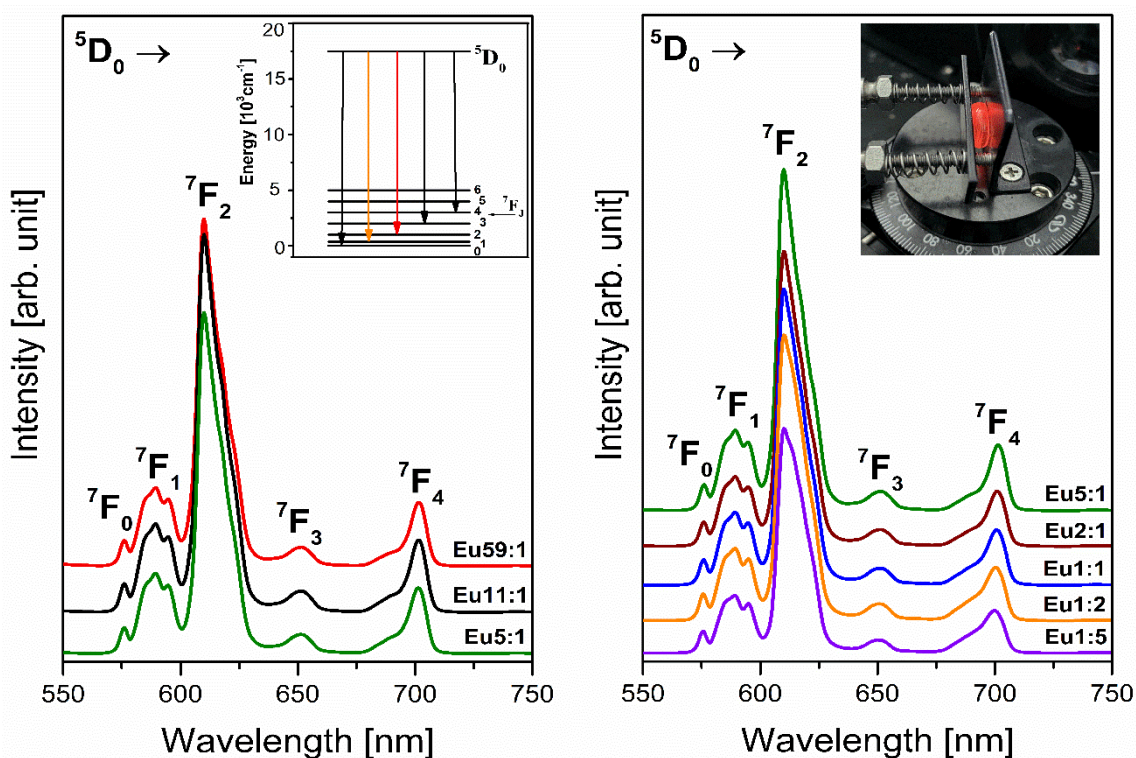


**Figure 6.** Emission spectra of  $\text{Eu}^{3+}$  ions doped glass samples with different concentrations of glass-former components ( $\text{GeO}_2$  and  $\text{B}_2\text{O}_3$ ). Insets present the emission transitions from the excited  $^5\text{D}_0$  level of lanthanide ions ( $\text{Eu}^{3+}$ ) and photographic image of glass sample under excitation of 396 nm.

As is generally known, the presence of all emission bands depends on the local centrosymmetry of  $\text{Eu}^{3+}$  ions in the studied glasses [57]. If trivalent europium ions in glass hosts are in a higher asymmetrical environment, the band related to transition  $^5\text{D}_0 \rightarrow ^7\text{F}_0$  could be recorded [58]. Moreover, the emission transitions  $^5\text{D}_0 \rightarrow ^7\text{F}_1$  and  $^5\text{D}_0 \rightarrow ^7\text{F}_2$ ,  $^5\text{D}_0 \rightarrow ^7\text{F}_4$  are allowed by magnetic and electric dipole interactions, respectively. It should be emphasized here that  $\text{Eu}^{3+}$  ions in the literature represent an attractive active dopant because, in addition to very efficient emission, they play an important role as a sensitive spectroscopic probe [59,60]. Two spectral ranges are relevant from this point of view.

The first range (580–600 nm) includes the band corresponding to the  $^5\text{D}_0 \rightarrow ^7\text{F}_1$  transition, and this transition follows the selection rule  $\Delta J = 1$ . However, the second range (602–636 nm) contains a band associated with the  $^5\text{D}_0 \rightarrow ^7\text{F}_2$  transition defined as a “hyper-sensitive” transition because the local environment strongly influences it and this transition

of  $\text{Eu}^{3+}$  ions follows the selection rule  $\Delta J = 2$ . Similar to the excitation spectra, the concentration of germanium dioxide is a critical factor determining the intensity of the narrow emission band associated with the  ${}^5\text{D}_0 \rightarrow {}^7\text{F}_2$  transition. This indicates that its intensity depends on the distortion (asymmetry) of the  $\text{Eu}^{3+}$  coordination polyhedron. The intensity of the band corresponding to the  ${}^5\text{D}_0 \rightarrow {}^7\text{F}_1$  transition is usually independent of the environment of the  $\text{Eu}^{3+}$  centers, which is also confirmed by the recorded emission spectra. For this reason, these transitions are fundamental in the analysis of the asymmetric ratio  $R/O = I({}^5\text{D}_0 \rightarrow {}^7\text{F}_2)/I({}^5\text{D}_0 \rightarrow {}^7\text{F}_1)$ . Considering the spectral range of these two transitions, the parameter  $R/O$  is also called the red-to-orange fluorescence intensity ratio of  $\text{Eu}^{3+}$  ions. In agreement with the literature, an appropriate selection of the oxides in glass compositions can influence the value of red-to-orange fluorescence intensity ratio of  $\text{Eu}^{3+}$  ions (Table 3). The reported results inform us about the local structure around the trivalent europium ions and the covalence degree of the  $\text{Eu}^{3+}-\text{O}^{2-}$  bond. The low value of the  $R/O$  ratio is usually attributed to the higher symmetry of the local environment around the  $\text{Eu}^{3+}$  ions. In contrast, an increase of the  $R/O$  value is due to an increase in the asymmetry of the local environment around the dopant ions [61,62]. The results of the conducted experiment showed an interesting correlation, which is shown in Figure 7a and Table 4.

Table 3. R/O-ratio values in various glass matrices.

Glass Composition [mol%]	R/O	References
10GeO <sub>2</sub> -50B <sub>2</sub> O <sub>3</sub> -30BaO-9.75Ga <sub>2</sub> O <sub>3</sub> -0.25Eu <sub>2</sub> O <sub>3</sub>	3.08	Present work
59GeO <sub>2</sub> -1B <sub>2</sub> O <sub>3</sub> -30BaO-9.75Ga <sub>2</sub> O <sub>3</sub> -0.25Eu <sub>2</sub> O <sub>3</sub>	3.63	Present work
89.5B <sub>2</sub> O <sub>3</sub> -10Li <sub>2</sub> O-0.5Eu <sub>2</sub> O <sub>3</sub>	2.41	[63]
0.5GeO <sub>2</sub> -63.5SiO <sub>2</sub> -16K <sub>2</sub> O-16BaO-4Eu <sub>2</sub> O <sub>3</sub>	3.46	[63]
84.5GeO <sub>2</sub> -12.5K <sub>2</sub> O-3Eu <sub>2</sub> O <sub>3</sub>	4.60	[63]
49.5BaO-49.5P <sub>2</sub> O <sub>5</sub> -1Eu <sub>2</sub> O <sub>3</sub>	5.28	[64]
30B <sub>2</sub> O <sub>3</sub> -40GeO <sub>2</sub> -29Gd <sub>2</sub> O <sub>3</sub> -1Eu <sub>2</sub> O <sub>3</sub>	3.54	[65]
25Sb <sub>2</sub> O <sub>3</sub> -25GeO <sub>2</sub> -29.2B <sub>2</sub> O <sub>3</sub> -5Al <sub>2</sub> O <sub>3</sub> -10Na <sub>2</sub> O-0.6AgNO <sub>3</sub> -0.2Eu <sub>2</sub> O <sub>3</sub>	2.75	[66]
45P <sub>2</sub> O <sub>5</sub> -45PbO-9Ga <sub>2</sub> O <sub>3</sub> -1Eu <sub>2</sub> O <sub>3</sub>	1.70	[67]
44P <sub>2</sub> O <sub>5</sub> -17K <sub>2</sub> O-9Al <sub>2</sub> O <sub>3</sub> -23PbF <sub>2</sub> -6Na <sub>2</sub> O-1Eu <sub>2</sub> O <sub>3</sub>	2.36	[68]
10Li <sub>2</sub> O-10PbO-7Al <sub>2</sub> O <sub>3</sub> -70B <sub>2</sub> O <sub>3</sub> -3Eu <sub>2</sub> O <sub>3</sub>	2.02	[69]
59.8GeO <sub>2</sub> -15Ga <sub>2</sub> O <sub>3</sub> -25BaO-0.2Eu <sub>2</sub> O <sub>3</sub>	3.72	[70]

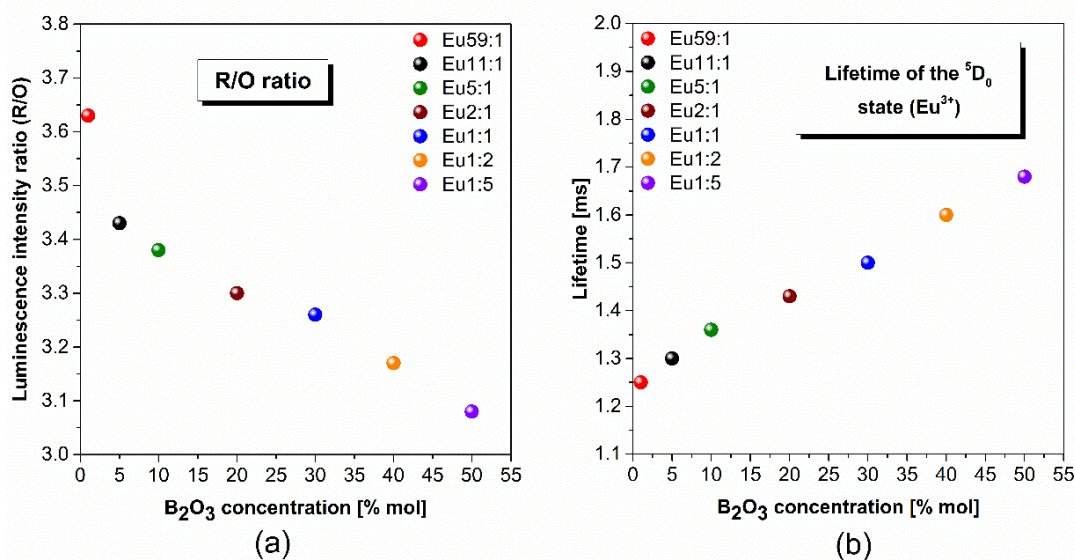


Figure 7. (a) Asymmetric ratio and (b) luminescence lifetime of obtained glass samples doped with trivalent europium ions containing extremely different glass-formers concentrations.

**Table 4.** R/O parameter and lifetimes calculated for glass samples doped with  $\text{Eu}^{3+}$  ions.

Sample Code	$\text{GeO}_2:\text{B}_2\text{O}_3$ [mol%]	R/O ( $\text{Eu}^{3+}$ )	$\tau_m$ [ms]
Eu59:1	59:1	3.63	1.25
Eu11:1	55:5	3.43	1.30
Eu5:1	50:10	3.38	1.36
Eu2:1	40:20	3.30	1.43
Eu1:1	30:30	3.26	1.50
Eu1:2	20:40	3.17	1.60
Eu1:5	10:50	3.08	1.68

The R/O ratio of the prepared systems with two glass-formers was found to have a minimum of 3.08 for the glass sample containing the predominant concentration of  $\text{B}_2\text{O}_3$  (Eu1:5). Interestingly, as a function of increasing germanium dioxide concentration, the value of R/O parameter is a maximum of 3.63. Therefore, the local symmetry around the  $\text{Eu}^{3+}$  ions and ionic character of  $\text{Eu}^{3+}-\text{O}^{2-}$  bond increases with the change in the molar ratio  $\text{GeO}_2:\text{B}_2\text{O}_3$  (from Eu59:1 to Eu1:5). The observed differences in the local environment around trivalent europium ions are due to the quantitative relationship of the two different glass-former oxides, which act as a more network-former or network-modifier component depending on the concentration.

Based on luminescence decay curves of the  $^5\text{D}_0$  level of  $\text{Eu}^{3+}$  ions in glass systems with two glass-formers  $\text{GeO}_2$  and  $\text{B}_2\text{O}_3$ , the luminescence lifetimes were determined. Another notable observation of the consequence of the change in the molar ratio ( $\text{GeO}_2:\text{B}_2\text{O}_3$ ) is schematized in Figure 7b and Table 4. In the studied glasses, the luminescence lifetime from upper excitation state  $^5\text{D}_0$  of trivalent europium increased in the direction from 1.25 ms to 1.68 ms for samples Eu59:1 and Eu1:5, respectively.

Analyzing the composition of obtained glass systems doped with  $\text{Eu}^{3+}$  ions, it can be stated that due to a higher concentration of boron trioxide, the lifetime for the  $^5\text{D}_0$  level is getting longer. Venkatramu et al. [71] reported that the decrease in the luminescence lifetime of the  $^5\text{D}_0$  in borate glasses is attributed to the electronegativities of the modifying oxide metals. Simultaneously, in the case of our study, the value of electronegativity Ge and B are comparable, therefore this factor does not significantly affect the luminescence lifetime. It was found that the observed decreasing tendency of a lifetime of the  $^5\text{D}_0$  level of  $\text{Eu}^{3+}$  ions is the effect of the phonon energy of the glassy matrix. From the literature data it is experimentally proved that when the phonon energy of the matrix is higher, there is a higher probability of non-radiative relaxation multiphonon processes, which may result in a reduction of luminescence lifetime for lanthanide ions [72]. A completely opposite relationship was observed, although systems with  $\text{B}_2\text{O}_3$  as glass-former have higher phonon energy than glasses with  $\text{GeO}_2$ . In this case, radiative relaxation from the excited levels of trivalent europium ions is dominant due to the very large energy gap between the  $^5\text{D}_0$  and  $^7\text{F}_6$  energy states of  $\text{Eu}^{3+}$  ions ( $\Delta E = 12,500 \text{ cm}^{-1}$ ). Consequently, more phonons are required for non-radiative relaxation multiphonon processes in studied systems with glass-former  $\text{GeO}_2$  than samples with  $\text{B}_2\text{O}_3$ . Previous experimental results proved this phenomenon because low-phonon germanate glasses doped with  $\text{Eu}^{3+}$  ions indicated relatively low luminescence lifetime values, 1.43 ms [73], 1.22 ms [74]. It is worth noting that the same parameter determined for high-phonon borate glasses was evaluated at 2.57 ms [75], 2.25 ms [76]. Moreover, the variations in the spectroscopic parameters—the decrease in the R/O ratio and the increase in the lifetimes with increasing  $\text{B}_2\text{O}_3$  and  $\text{GeO}_2$ —correlate with the changes in the intensity of the emission bands. The obtained results confirmed the research question of the authors' investigations and indicated the critical role of glass-former in spectroscopic properties of systems that may find potential use as optical materials.

#### 4. Conclusions

In the present work, GeO<sub>2</sub>-B<sub>2</sub>O<sub>3</sub>-BaO-Ga<sub>2</sub>O<sub>3</sub> glass systems singly doped with transition metals (Cr<sup>3+</sup>) and lanthanides (Eu<sup>3+</sup>) were prepared by high-temperature melt-quenching method. The proposed modification of the concentration of the two main glass-formers components provided the following conclusions:

- Analysis of EPR spectra indicates that the trivalent chromium ions at octahedral sites are present in the glass network. Independently of the molar ratio of different glass-formers, red luminescence was observed for systems doped with Cr<sup>3+</sup> ions in octahedral sites. The influence of changing concentration glass-formers on the intensity of R-line attributed to Cr<sup>3+</sup> ions in high-field sites was proved. It was stated that the emission bands with maxima at about 780 nm and 1070 nm are related to the same transition (<sup>4</sup>T<sub>2</sub> → <sup>4</sup>A<sub>2</sub>) of trivalent chromium ions in octahedral and tetrahedral sites, respectively.
- Confirmation that the type of glass-formers has a significant contribution to the properties of amorphous materials is presented by the results of spectroscopic studies conducted for glass samples doped with Eu<sup>3+</sup> ions. Detailed spectroscopic analysis of the emission spectra showed a gradual quenching of the luminescence as a function of boron oxide concentration. The obtained values of the ratio R indicate a more covalent nature of the bond between the lanthanide ions and the surrounding ligands for samples with a higher concentration of germanium dioxide. On the other hand, the increase in boron oxide concentration results in an increase in the values of luminescence lifetimes of <sup>5</sup>D<sub>0</sub> level of Eu<sup>3+</sup> ions.

In summary, the results presented in this manuscript demonstrate that spectroscopic properties of systems doped with transition metal and lanthanides ions should be controlled by the choice of glass-formers. The developed oxide glasses emit efficient radiation in the visible and near-infrared range. From the application point of view, the prepared glasses can be classified as interesting and useful optical materials for potential application in the field of photonics.

**Author Contributions:** Conceptualization, W.A.P.; methodology, J.P. (Joanna Pisarska) and W.A.P.; formal analysis, K.K., M.K. and W.A.P.; investigation, K.K., M.K. and J.P. (Justyna Polak); writing—original draft preparation, K.K. and M.K.; writing—review and editing, W.A.P.; visualization, K.K. and M.K. All authors have read and agreed to the published version of the manuscript.

**Funding:** This research received no external funding.

**Institutional Review Board Statement:** Not applicable.

**Informed Consent Statement:** Not applicable.

**Data Availability Statement:** Not applicable.

**Acknowledgments:** Publication co-financed by the funds granted under the Research Excellence Initiative of the University of Silesia in Katowice.

**Conflicts of Interest:** The authors declare no conflict of interest.

#### References

1. Pascuta, P.; Stefan, R.; Olar, L.E.; Bolundut, L.C.; Culea, E. Effects of Copper Metallic Nanoparticles on Structural and Optical Properties of Antimony Phosphate Glasses Co-Doped with Samarium Ions. *Materials* **2020**, *13*, 5040. [[CrossRef](#)]
2. Hongisto, M.; Veber, A.; Petit, Y.; Cardinal, T.; Danto, S.; Jubera, V.; Petit, L. Radiation-Induced Defects and Effects in Germanate and Tellurite Glasses. *Materials* **2020**, *13*, 3846. [[CrossRef](#)]
3. Østergaard, M.B.; Bødker, M.S.; Smedskjaer, M.M. Structure Dependence of Poisson's Ratio in Cesium Silicate and Borate Glasses. *Materials* **2020**, *13*, 2837. [[CrossRef](#)]
4. Wang, X.; Sakakura, M.; Liu, Y.; Qiu, J.; Shimotsuma, Y.; Hirao, K.; Miura, K. Modification of long range order in germanate glass by ultra fast laser. *Chem. Phys. Lett.* **2011**, *511*, 266–269. [[CrossRef](#)]
5. Zanutto, E.D.; Mauro, J.C. The glassy state of matter: Its definition and ultimate fate. *J. Non-Cryst. Solids* **2017**, *471*, 490–495. [[CrossRef](#)]
6. Zachariasen, W.H. The atomic arrangement in glass. *J. Am. Chem. Soc.* **1932**, *54*, 3841–3851. [[CrossRef](#)]

7. Laksminarayana, G.; Meza-Rocha, A.N.; Soriano-Romeo, O.; Huerta, E.F.; Caldino, U.; Lira, A.; Lee, D.-E.; Yoon, J.; Park, T. Analysis of fluorescence characteristics of Sm<sup>3+</sup>-doped B<sub>2</sub>O<sub>3</sub>-rich glasses for Orange-light-emitting diodes. *J. Alloys Compd.* **2021**, *884*, 161076. [[CrossRef](#)]
8. Fan, X.; Zhang, W.; Lu, F.; Sui, Y.; Wang, J.; Xu, Z. Research of Fluorescent Properties of a New Type of Phosphor with Mn<sup>2+</sup>-Doped Ca<sub>2</sub>SiO<sub>4</sub>. *Sensors* **2021**, *21*, 2788. [[CrossRef](#)]
9. Tanabe, S. Rare-earth-doped glasses for fiber amplifiers in broadband telecommunication. *Comptes Rendus Chim.* **2002**, *5*, 815–824. [[CrossRef](#)]
10. Zaini, N.A.; Mohamed, S.N.; Mohamed, Z. Effects of Vanadium on the Structural and Optical Properties of Borate Glasses Containing Er<sup>3+</sup> and Silver Nanoparticles. *Materials* **2021**, *14*, 3710. [[CrossRef](#)]
11. Veselský, K.; Lahti, V.; Petit, L.; Prajzler, V.; Šulc, J.; Jelínková, H. Influence of Y<sub>2</sub>O<sub>3</sub> Content on Structural, Optical, Spectroscopic, and Laser Properties of Er<sup>3+</sup>, Yb<sup>3+</sup> Co-Doped Phosphate Glasses. *Materials* **2021**, *14*, 4041. [[CrossRef](#)] [[PubMed](#)]
12. Santos Barbosa, J.; Batista, G.; Danto, S.; Fargin, E.; Cardinal, T.; Poirier, G.; Castro Cassanjes, F. Transparent Glasses and Glass-Ceramics in the Ternary System TeO<sub>2</sub>-Nb<sub>2</sub>O<sub>5</sub>-PbF<sub>2</sub>. *Materials* **2021**, *14*, 317. [[CrossRef](#)] [[PubMed](#)]
13. Yue, Y.; Shao, C.; Kang, S.; Wang, F.; Wang, X.; Ren, J.; He, D.; Chen, W.; Hu, L. Investigation of luminescence mechanism of Nd<sup>3+</sup>-doped calcium aluminate glasses: Effect of glass-formers. *J. Non-Cryst. Solids* **2019**, *505*, 333–339. [[CrossRef](#)]
14. Kuusela, L.; Veber, A.; Boetti, N.G.; Petit, L. Impact of ZnO Addition on Er<sup>3+</sup> Near-Infrared Emission, the Formation of Ag Nanoparticles, and the Crystallization of Sodium Fluorophosphate Glass. *Materials* **2020**, *13*, 527. [[CrossRef](#)]
15. Liu, R.; Chen, M.; Zhu, X.; Zhu, Y.; Zeng, F.; Su, Z. Luminescent properties and structure of Dy<sup>3+</sup> doped germanosilicate glass. *J. Lumin.* **2020**, *226*, 117378. [[CrossRef](#)]
16. Jiao, Q.; Li, G.; Zhou, D.; Qiu, J. Effect of the Glass Structure on Emission of Rare-Earth-Doped Borate Glass. *J. Am. Ceram. Soc.* **2015**, *98*, 4102–4106. [[CrossRef](#)]
17. Herrmann, A.; Kuhn, S.; Tiegel, M.; Russel, C. Fluorescence properties of Eu<sup>3+</sup>-doped alumino silicate glasses. *Opt. Mater.* **2014**, *37*, 293–297. [[CrossRef](#)]
18. Linganna, K.; Narro-Garcia, R.; Desirens, H.; De la Rosa, E.; Basavapoornima, C.; Venkatramu, V.; Jayasankar, C.K. Effect of P<sub>2</sub>O<sub>5</sub> addition on structural and luminescence properties of Nd<sup>3+</sup>-doped tellurite glasses. *J. Alloys Compd.* **2016**, *684*, 322–327. [[CrossRef](#)]
19. Marzouk, M.A. Optical characterization of some rare earth ions doped bismuth borate glasses and effect of gamma irradiation. *J. Mol. Struct.* **2012**, *1019*, 80–90. [[CrossRef](#)]
20. Divina, R.; Evangelin Teresa, P.; Marimuthu, K. Dy<sup>3+</sup> ion as optical probe to study the luminescence behavior of Alkali lead bismuth borate glasses for w-LED application. *J. Alloys Compd.* **2021**, *883*, 160845. [[CrossRef](#)]
21. Djamal, M.; Yuliantini, L.; Hidayat, R.; Rauf, N.; Horprathum, M.; Rajaramakrishna, R.; Boonin, K.; Yasaka, P.; Kaewkhao, J.; Venkatramu, V.; et al. Spectroscopic study of Nd<sup>3+</sup> ion-doped Zn-Al-Ba borate glasses for NIR emitting device applications. *Opt. Mater.* **2020**, *107*, 110018. [[CrossRef](#)]
22. Pisarska, J.; Pisarski, W.A.; Lisiecki, R.; Ryba-Romanowski, W. Phonon Sideband Analysis and Near-Infrared Emission in Heavy Metal Oxide Glasses. *Materials* **2021**, *14*, 121. [[CrossRef](#)] [[PubMed](#)]
23. Pipes, R.S.; Shelby, J.E. Formation and properties of soda lime germanate glasses. *J. Non-Cryst. Solids* **2021**, *553*, 120506. [[CrossRef](#)]
24. Koroleva, O.N.; Shtenberg, M.V.; Ivanova, T.N. The structure of potassium germanate glasses as revealed by Raman and IR spectroscopy. *J. Non-Cryst. Solids* **2010**, *510*, 143–150. [[CrossRef](#)]
25. Zmojda, J.; Kochanowicz, M.; Miluski, P.; Golonko, P.; Baranowska, A.; Ragiń, T.; Dorosz, J.; Kuwik, M.; Pisarski, W.; Pisarska, J.; et al. Luminescent Studies on Germanate Glasses Doped with Europium Ions for Photonics Applications. *Materials* **2020**, *13*, 2817. [[CrossRef](#)]
26. Pisarski, W.A.; Kowalska, K.; Kuwik, M.; Polak, J.; Pietrasik, E.; Goryczka, T.; Pisarska, J. Novel Multicomponent Titanate-Germanate Glasses: Synthesis, Structure, Properties, Transition Metal, and Rare Earth Doping. *Materials* **2020**, *13*, 4422. [[CrossRef](#)]
27. Tanaka, M.; Kushida, T. Studies of the vibronic interaction between Eu<sup>3+</sup> ions and glass-forming units in oxide glasses. *Chem. Phys. Lett.* **1999**, *315*, 428–432. [[CrossRef](#)]
28. Rolli, R.; Camagni, P.; Samoggia, G.; Speghini, A.; Wachtler, M.; Bettinelli, M. Fluorescence line narrowing spectroscopy of a lead germanate glass doped with Eu<sup>3+</sup>. *Spectrochim. Acta Part A* **1998**, *54*, 2157–2162. [[CrossRef](#)]
29. Hanyes, W.M. *CRC Handbook of Chemistry and Physics*, 93rd ed.; CRC Press: Boca Raton, FL, USA, 2004; pp. 4–13.
30. Binnemans, K. Interpretation of europium (III) spectra. *Coord. Chem. Rev.* **2015**, *295*, 1–45. [[CrossRef](#)]
31. Fujihara, S.; Shibata, Y. Luminescence of Cr<sup>3+</sup> ions associated with surpassing the green-emissive defect centers in B-Ga<sub>2</sub>O<sub>3</sub>. *J. Lumin.* **2006**, *121*, 470–474. [[CrossRef](#)]
32. Rasheed, F.; O'Donnell, K.P.; Henderson, B.; Hollis, D.B. Disorder and the optical spectroscopy of Cr<sup>3+</sup>-doped glasses: I. Silicate glasses. *J. Phys. Condens. Matter* **1991**, *3*, 1915–1930. [[CrossRef](#)]
33. Rossi, F.; Montagna, M.; Ferrari, M.; Capobianco, J.A.; Bettinelli, M. Line width measurements of Cr<sup>3+</sup> in a zinc borate glass. *J. Non-Cryst. Solids* **1998**, *240*, 232–236. [[CrossRef](#)]
34. Samdani, M.; Ramadevudu, G.; Narasimha Chary, M.; Shareefuddin, M. EPR, optical and physical studies on Cr<sup>3+</sup> doped MgO-BaO-B<sub>2</sub>O<sub>3</sub>-TeO<sub>2</sub> glasses. *St. Petersburg Polytech. Univ. J. Phys. Math.* **2017**, *3*, 299–307.
35. Costa, V.C.; Lameiras, F.S.; Pinheiro, M.V.B.; Sousa, D.F.; Nunes, L.A.O.; Shen, Y.R.; Bray, K.L. Laser spectroscopy and electron paramagnetic resonance of Cr<sup>3+</sup> doped silicate glasses. *J. Non-Cryst. Solids* **2000**, *273*, 209–214. [[CrossRef](#)]

36. Samdani; Ramadevudu, G.; Narasimha Chary, M.; Shareefuddin, M. Physical and spectroscopic studies of Cr<sup>3+</sup> doped mixed alkaline earth oxide borate glasses. *Mater. Chem. Phys.* **2017**, *186*, 382–389. [[CrossRef](#)]
37. Santhan Kumar, J.; Lakshmi Kumari, J.; Subba Rao, M.; Cole, S. EPR, optical and physical properties of chromium ions in CdO-SrO-B<sub>2</sub>O<sub>3</sub>-SiO<sub>2</sub> (CdSBSi) glasses. *Opt. Mater.* **2013**, *35*, 1320–1326. [[CrossRef](#)]
38. Bala Murali Krishna, S.; Vinaya Teja, P.M.; Krishna Rao, D. Role of chromium ion valence states in ZnO-As<sub>2</sub>O<sub>3</sub>-Sb<sub>2</sub>O<sub>3</sub> glass system by means of spectroscopic and dielectric studies. *Mater. Res. Bull.* **2010**, *45*, 1783–1791. [[CrossRef](#)]
39. Kesavulu, C.R.; Chakradhar, R.P.S.; Muralidhara, R.S.; Rao, J.L.; Anavekar, R.V. EPR, optical absorption and photoluminescence properties of Cr<sup>3+</sup> ions in lithium borophosphate glasses. *J. Alloys Compd.* **2010**, *496*, 75–80. [[CrossRef](#)]
40. Babkina, A.; Valiev, D.; Zyryanova, K.; Nuryev, R.; Ignatiev, A.; Kulpina, E.; Kuzmenko, N.; Osipova, A.; Koroleva, A.; Platonova, N. Spectroscopic properties of chromium/antimony co-doped alkali-alumina-borate glass-ceramics. *Opt. Mater.* **2020**, *106*, 109983. [[CrossRef](#)]
41. Kiran, N.; Kesavulu, C.R.; Suresh Kumar, A.; Rao, J.L. Spectral studies on Cr<sup>3+</sup> ions doped in sodium-lead borophosphate glasses. *Phys. B* **2011**, *406*, 1897–1901. [[CrossRef](#)]
42. Wen, H.; Xie, S.; Cui, J.; Mao, S.; Luo, L.; Brik, M.G. Optical properties of 3d transition metal ion-doped aluminophosphate glasses. *J. Lumin.* **2019**, *213*, 263–272. [[CrossRef](#)]
43. Saad, N.; Haouari, M.; Bulou, A.; HadiKassiba, A.; Ben Ouada, H. Structural and optical properties of Cr<sup>3+</sup> embedded in a P<sub>2</sub>O<sub>5</sub>-B<sub>2</sub>O<sub>3</sub>-ZnO-BaF<sub>2</sub>-AlF<sub>3</sub> fluoroborophosphate glasses. *Mater. Chem. Phys.* **2018**, *212*, 461–470. [[CrossRef](#)]
44. Rodríguez-Mendoza, U.R.; Speghini, A.; Jaque, D.; Zambelli, M.; Bettinelli, M. Optical properties of single doped Cr<sup>3+</sup> and co-doped Cr<sup>3+</sup>-Nd<sup>3+</sup> aluminum tantalum tellurite glasses. *J. Alloys Compd.* **2004**, *380*, 163–166. [[CrossRef](#)]
45. Narendrudu, T.; Suresh, S.; Chinna Ram, G.; Veeraiah, N.; Krishna Rao, D. Spectroscopic and structural properties of Cr<sup>3+</sup> ions in lead niobium germanosilicate glasses. *J. Lumin.* **2017**, *183*, 17–25. [[CrossRef](#)]
46. Yang, X.I.; Wang, W.C.; Zhang, Q.Y. BaF<sub>2</sub> modified Cr<sup>3+</sup>/Ho<sup>3+</sup> co-doped germanate glass for efficient 2.0 μm fiber lasers. *J. Non-Cryst. Solids* **2018**, *482*, 147–153. [[CrossRef](#)]
47. Mikulski, J.; Koepke, C.; Wiśniewski, K.; Padlyak, B.V.; Adamiv, V.T.; Burak, Y.V. Excited state characteristics of the Li<sub>2</sub>B<sub>4</sub>O<sub>7</sub> and KLiB<sub>4</sub>O<sub>7</sub> glasses active by Cr<sup>3+</sup> ions. *Opt. Mater.* **2014**, *38*, 24–27. [[CrossRef](#)]
48. Li, Y.; Ye, S.; Zhang, Q. Ultra-broadband near-infrared luminescence of ordered-disordered multi-sited Cr<sup>3+</sup> in La<sub>3</sub>Ga<sub>5.5</sub>Nb<sub>0.5</sub>O<sub>14</sub>:Cr<sup>3+</sup>. *J. Mater. Chem. C* **2014**, *2*, 4636–4641. [[CrossRef](#)]
49. Babu, P.; Jayasankar, C.K. Optical spectroscopy of Eu<sup>3+</sup> ions in lithium borate and lithium fluoroborate glasses. *Phys. B* **2000**, *279*, 262–281. [[CrossRef](#)]
50. Ramesh, P.; Hegde, V.; Pramod, A.G.; Eraiah, B.; Agarkov, D.A.; Eliseeva, G.M.; Pandey, M.K.; Annapurna, K.; Jagannath, G.; Kokila, M.K. Compositional dependence of red photoluminescence of Eu<sup>3+</sup> ions in lead and bismuth containing borate glasses. *Solid State Sci.* **2020**, *107*, 106360. [[CrossRef](#)]
51. Fabian, M.; Pinakidou, F.; Tolnai, I.; Czompoly, O.; Osan, J. Lanthanide (Ce, Nd, Eu) environments and leaching behavior in borosilicate glasses. *Sci. Rep.* **2021**, *11*, 13272. [[CrossRef](#)]
52. Wang, B.; Li, D.S.; Shen, L.F.; Pun, E.Y.B.; Lin, H. Eu<sup>3+</sup> doped high-brightness fluorophosphate laser-driven glass phosphors. *Opt. Mater. Exp.* **2019**, *9*, 1749–1762. [[CrossRef](#)]
53. Mahato, K.K.; Rai, S.B.; Rai, A. Optical studies of Eu<sup>3+</sup> doped oxyfluoroborate glass. *Spectrochim. Acta Part A Mol. Biomol. Spectrosc.* **2004**, *60*, 979–985. [[CrossRef](#)]
54. Rodriguez, V.D.; Lavin, V.; Rodriguez-Mendoza, U.R.; Martin, I.R. Spectroscopy of rare earth ions in fluoride glasses for laser applications. *Opt. Mater.* **1999**, *13*, 1–7. [[CrossRef](#)]
55. Han, L.; Zhang, Q.; Song, J.; Xiao, Z.; Qiang, Y.; Ye, X.; You, W.; Lu, A. A novel Eu<sup>3+</sup>-doped phosphate glass for reddish orange emission: Preparation, structure and fluorescence properties. *J. Lumin.* **2020**, *221*, 117041. [[CrossRef](#)]
56. Aryal, P.; Kim, H.J.; Khan, A.; Saha, S.; Kang, S.J.; Kothan, S.; Yamsuk, Y.; Kaewkhao, J. Development of Eu<sup>3+</sup>-doped phosphate glass. For luminescent solid-state optical devices. *J. Lumin.* **2020**, *227*, 117564. [[CrossRef](#)]
57. Chen, M.; Liu, R.; Wang, D.; Zhou, Y.; Zeng, F.; Su, Z. Luminescent properties of Eu<sup>3+</sup> doped germanosilicate red glass. *J. Non-Cryst. Solids* **2021**, *566*, 120895. [[CrossRef](#)]
58. Balda, R.; Fernandez, J.; Duhamel, N.; Adam, J.L.; Imbusch, G.F. Site-selection spectroscopy and energy transfer studies of Eu<sup>3+</sup> ions in a new fluorophosphate glass. *J. Lumin.* **1995**, *66–67*, 290–293. [[CrossRef](#)]
59. Cascales, C.; Balda, R.; Garcia-Revilla, S.; Lezama, L.; Barredo-Zuriarrain, M.; Fernandez, J. Site symmetry and host-sensitization-dependence of Eu<sup>3+</sup> real time luminescence in tin dioxide nanoparticles. *Opt. Exp.* **2018**, *26*, 16155–16170. [[CrossRef](#)]
60. Wen, H.; Jia, G.; Duan, C.K.; Tanner, P.A. Understanding Eu<sup>3+</sup> emission spectra in glass. *Phys. Chem. Chem. Phys.* **2010**, *12*, 9933–9937. [[CrossRef](#)]
61. De, M.; Jana, S. Optical characterization of Eu<sup>3+</sup> doped titanium barium lead phosphate glass. *Optik* **2020**, *215*, 164718. [[CrossRef](#)]
62. Mariselvam, K.; Arun Kumar, R.; Karthik, S. Optical and luminescence characteristics of europium doped barium lithium fluoroborate glasses. *Chem. Phys.* **2019**, *525*, 110379. [[CrossRef](#)]
63. Oomen, E.W.J.L.; van Dongen, A.M.A. Europium (III) in oxide glasses: Dependence of the emission spectrum upon glass composition. *J. Non-Cryst. Solids* **1989**, *111*, 205–213. [[CrossRef](#)]
64. Reisfeld, R.; Boehm, L.; Ish-Shalom, M.; Fischer, R. 4f yields 4f transitions and charge transfer spectra of Eu<sup>3+</sup>, 4f yields 5d spectra of Tb<sup>3+</sup>, and <sup>1</sup>S<sub>0</sub> yields <sup>3</sup>P<sub>1</sub> spectra of Pb<sup>2+</sup> in alkaline earth metaphosphate glasses. *Phys. Chem. Glasses* **1974**, *15*, 76.

65. Gokce, M.; Senturk, U.; Uslu, D.K.; Burgaz, G.; Sahin, Y.; Gokce, A.G. Investigation of europium concentration dependence on the luminescent dependence on the luminescent properties of borogermanate glasses. *J. Lumin.* **2017**, *192*, 263–268. [[CrossRef](#)]
66. Zmoja, J.; Kochanowicz, M.; Miluski, P.; Baranowska, A.; Pisarski, W.A.; Pisarska, J.; Jadach, R.; Sitarz, M.; Dorosz, D. Structural and optical properties of antimony-germanate-borate glass and glass fiber co-doped  $\text{Eu}^{3+}$  and Ag nanoparticles. *Spectrochim. Acta A Mol. Biomol. Spectrosc.* **2018**, *201*, 1–7. [[CrossRef](#)]
67. Sołtys, M.; Janek, J.; Zur, L.; Pisarska, J.; Pisarski, W.A. Compositional-dependent europium-doped lead phosphate glasses and their spectroscopic properties. *Opt. Mater.* **2015**, *40*, 91–96. [[CrossRef](#)]
68. Kesavulu, C.R.; Kumar, K.K.; Vijaya, N.; Lim, K.S.; Jayasankar, C.K. Thermal vibration and optical properties of  $\text{Eu}^{3+}$ -doped lead fluorophosphate glasses for red laser applications. *Mater. Chem. Phys.* **2013**, *141*, 903–911. [[CrossRef](#)]
69. Deopa, N.; Kaur, S.; Prasad, A.; Joshi, B.; Rao, A.S. Spectral studies of  $\text{Eu}^{3+}$  doped lithium lead alumino borate glasses for visible photonic applications. *Opt. Laser Technol.* **2018**, *108*, 434–440. [[CrossRef](#)]
70. Szal, R.; Zmoja, J.; Kochanowicz, M.; Miluski, P.; Dorosz, J.; Lesniak, M.; Jeleń, P.; Starzyk, B.; Sitarz, M.; Kuwik, M.; et al. Spectroscopic properties of antimony modified germanate glass doped with  $\text{Eu}^{3+}$  ions. *Ceram. Int.* **2019**, *45*, 24811–24817. [[CrossRef](#)]
71. Venkatramu, V.; Babu, P.; Jayasankar, C.K. Fluorescence properties of  $\text{Eu}^{3+}$  ions doped borate and fluoroborate glasses containing lithium, zinc and lead. *Spectrochim. Acta A Mol. Biomol. Spectrosc.* **2006**, *63*, 276–281. [[CrossRef](#)]
72. Shojiya, M.; Kawamoto, Y. Judd-Ofelt parameters and multiphonon relaxation of  $\text{Ho}^{3+}$  ions in  $\text{ZnCl}_2$ -based glass. *J. Appl. Phys.* **2001**, *89*, 4944–4950. [[CrossRef](#)]
73. Wang, X.; Huang, L.; Zhao, S.; Xu, S.  $\text{Eu}^{3+}$  doped heavy germanate scintillating glasses. *J. Lumin.* **2018**, *196*, 256–258. [[CrossRef](#)]
74. Zur, L.; Janek, J.; Pietrasik, E.; Sołtys, M.; Pisarska, J.; Pisarski, W.A. Influence of  $\text{Mo}/\text{MF}_2$  modifiers ( $\text{M} = \text{Ca}, \text{Sr}, \text{Ba}$ ) on spectroscopic properties of  $\text{Eu}^{3+}$  ions in germanate and borate glasses. *Opt. Mater.* **2016**, *61*, 59–63. [[CrossRef](#)]
75. Vijayalakshmi, L.; Kumar, K.N.; Hwang, P. Dazzling red luminescence dynamics of  $\text{Eu}^{3+}$  doped lithium borate glasses for photonic applications. *Optic* **2019**, *193*, 163019. [[CrossRef](#)]
76. Yao, L.; Chen, G.; Cui, S.; Zhong, H.; Wen, C. Fluorescence and optical properties of  $\text{Eu}^{3+}$ -doped borate glasses. *J. Non-Cryst. Solids* **2016**, *444*, 38–42. [[CrossRef](#)]